Self-assembled islands on strained systems: Control of formation, evolution, and spatial distribution

C. A. C. Mendonça, M. A. Cotta, E. A. Meneses, and M. M. G. Carvalho
UNICAMP, IFGW, DFA/LPD, Caixa Postal 6165, 13081-970, Campinas, S.P., Brazil
(Received 27 August 1997)

The dynamics of island formation on strained epitaxial films is investigated using the system formed by InAs on InP. Island shape, size, and spatial distribution are determined by surface atom diffusion that is modified by the presence of steps and/or corrugations on the surface. Different step characteristics—type and density—are shown to strongly affect the islanding process. By controlling the morphology of the underlying InP film we were able to achieve InAs/InP structures with periodic spatial distribution in one single step of growth. [S0163-1829(98)13619-6]

Low dimensionality of systems based on semiconductor materials has been investigated, theoretically and experimentally, as a means to improve the optical and electronic properties of structures and devices.[1,2] The fabrication of most of the systems in which carriers are confined in two or three directions—quantum wires and dots—has so far been based on quantum wells (QW's) and on the subsequent processing steps to produce arrays of one- and zero-dimensional structures.[3]

The achievement of high-quality interfaces, the most important feature of QW structures, has been one of the greatest challenges to the optimization of devices. Either for homointerfaces or heterointerfaces, the initial stage of growth has played a crucial role in the characteristics of the subsequent layers. The advance of surface and interface analysis techniques has made it possible to take a closer look at these interfaces at the very beginning of their formation, providing an understanding of the processes involved in the growth at this point. The natural consequences of this fact are a better control of the effects of growth parameters to obtain a desired interface and the possibility of creation of systems based on these processes.

Highly strained heterostructures[4–9] are examples of systems being investigated under this new light. In these systems the spontaneous formation of three-dimensional (3D) islands has been considered as a promising way to achieve arrays of self-organized quantum dots. However, the application of these structures on the fabrication of devices depends on the improvement of the control of island characteristics.

With regard to III-V compounds, In(Ga)As films grown on GaAs and on InP have been studied in the last few years. Island formation was shown to be controlled by the parameters that affect the diffusion of adatoms on the substrate surface, as substrate temperature and growth rate. It has also been observed that the accumulation of InAs in certain regions of the structures can be related to the presence of a strain field at the surface that is determinant to the process. Tersoff, Teichert, and Lagally[10] claim that the strain field creates a favorable region for nucleation while Xie *et al.*[11] discuss its effect on the diffusion of the adatoms at the surface. Both works focused on the achievement of vertically aligned InAs islands on multilayered InAs/GaAs structures.

The effect of step edges on island nucleation, investigated by Leonard, Pond, and Petroff,[12] suggests that different characteristics of the terraces and steps on the surface give rise to distinct diffusion dynamics, caused by alteration of the microscopic adatom hopping diffusion. Different morphologies of the buffer layer, created by *ex situ* processing, have been reported to affect island characteristics through modification of migration of adatoms on different crystal planes.[13,14] On the other hand, Kitamura *et al.* have shown that different misorientations of GaAs vicinal substrates did not modify the characteristics of $In_xGa_{1-x}As$ islands formed on multiatomic steps.[15,16] However, the critical thickness for 3D islanding of InP on GaAs has not varied for (100)-oriented substrates and 2° off this direction.[17]

In this work we report on the formation—in one step—of a spatially organized system of 3D InAs islands on InP, e.g., with no *ex situ* processing step and no need to grow a large number of layers. We discuss the process of InAs island formation on InP surfaces based on the alteration of the diffusion of the surface atoms due to temperature and due to the presence of steps and corrugation edges.

We observe that InAs islands tend to form in preferential regions of the surface and use this fact together with the possibility to create a surface with controlled morphology[18] to tailor the islands' spatial distribution. We also show that the size distribution of the InAs islands can be determined by carefully monitoring the cooling of the samples.

We use in-air atomic force microscopy (AFM) of InAs films at the earliest stages of their deposition on InP to investigate the dependence of the 3D islanding process on substrate misorientation and morphology of the InP buffer layer. The samples investigated in this work were grown by chemical beam epitaxy using trimethylindium diluted with hydrogen carrier gas as the group-III source and thermally decomposed pure arsine (AsH_3) and phosphine (PH_3) as group-V sources. They consist of 2 ML of InAs deposited on 300 nm InP buffer layers. The deposition of InAs films was carried out at 0.7 ML/s, at 500 °C, with all structures being grown simultaneously on (100) InP substrates nominally oriented and 2° off towards [011] (*A* surface), [011] (*B* surface), and [101] (*C* surface) directions. The substrate temperature was monitored by standard infrared pyrometry. The morphology

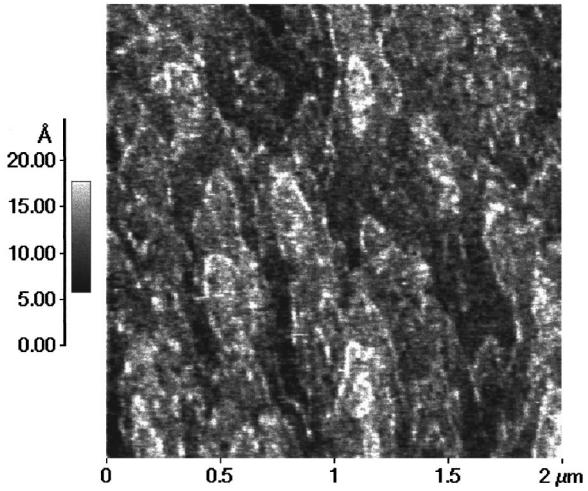

FIG. 1. AFM image of 2 ML InAs films grown on nominal (100) substrate with $\Delta \mathbf{t} = 45$ s (scan size, $2 \times 2\ \mu m^2$).

of the InP buffer layers was intentionally varied from a smooth surface (2D growth mode) to a surface with a periodical multiterrace structure presenting a sawtooth profile along the [011] direction, which will hereafter be called the corrugated buffer. This profile corresponds to the formation of (411) sidewalls and occurs during the kinetic roughening of InP surfaces as described by Cotta *et al.*[18]

Different procedures were used after InAs deposition to evaluate the changes on island characteristics during the initial stages of the cooling of the samples. These procedures consist in allowing the samples to cool down under AsH_3 flux for different time intervals $\Delta \mathbf{t}$ before the deposition of a thin InP cap layer, after which the cooling process proceeds to room temperature under PH_3 flux.

In Fig. 1 we show the AFM image for an InAs film deposited on a smooth InP buffer layer grown on the nominal (100) substrate. For this sample $\Delta \mathbf{t} = 45$ s. Large 2D terraces are observed with well-defined 1-ML steps between them. The formation of 2D islands of InAs at the step edges can be clearly distinguished, suggesting a pinning effect at step edges during diffusion, as opposed to the case of lower growth temperatures for which 2D islands are randomly distributed on the top of the terraces.[16] These terraces are not seen at the samples grown on the other types of substrate due to smaller terrace width, which is beyond AFM resolution, limiting the observation to larger structures.

As far as misoriented substrates are concerned we will discuss samples grown on *A* and *C* surfaces. The main difference between these two is that in the former only *A* steps are present while *A* and *B* steps coexist on the *C* surface. We will also restrict our analysis to those films grown on *C* surfaces, as representative of the surfaces with *B* steps, due to the similarity of the results obtained for these samples compared to those grown on B-type substrates.

Figures 2(a) and 2(b) show the AFM results for films deposited on *A*- and *C*-type substrates, respectively. These samples were grown on the same run as that shown in Fig. 1, i.e., $\Delta \mathbf{t} = 45$ s. Three-dimensional islands can be observed on the *C* substrate [Fig. 2(b)], while no island is distinguished on the AFM images of the sample on the *A* surface. This fact indicates that the InAs nucleation and islanding begins earlier for films grown on *C* substrates. In Figs. 2(c) and 2(d) we show the AFM images of samples in which $\Delta \mathbf{t} = 120$ s, on *A*- and *C*-type substrates, respectively. Under these conditions, AFM images of samples grown on the *A* surface also show the presence of 3D islands. Some of them are elongated along the direction [011], their shape suggesting the coalescence of smaller islands. Islands on the *C* surface, on

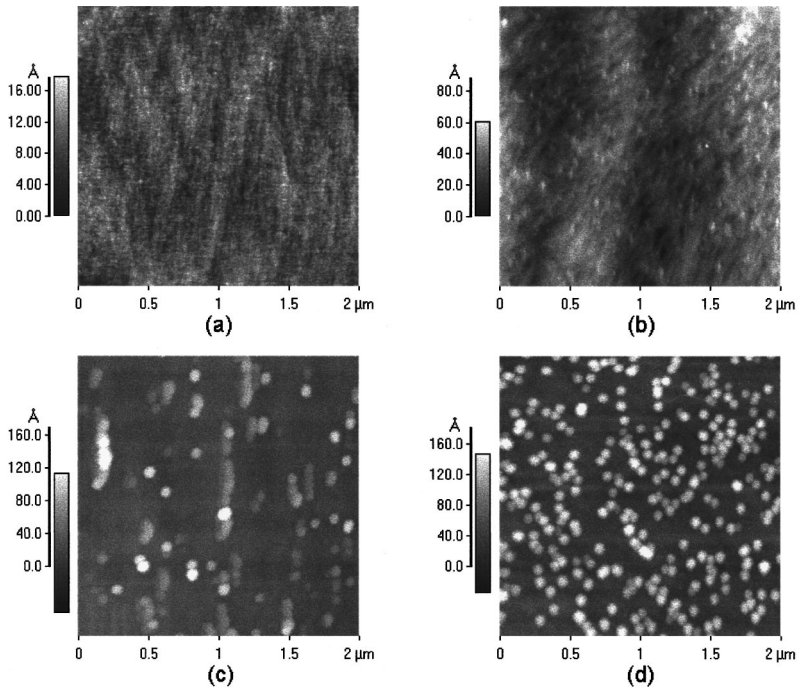

FIG. 2. AFM images of 2 ML InAs films deposited on (a) *A* surface and (b) *C* surfaces, with $\Delta \mathbf{t} = 45$ s, respectively. (c) *A* surface and (d) *C* surface, respectively, with $\Delta \mathbf{t} = 120$ s (scan size, $2 \times 2\ \mu m^2$).

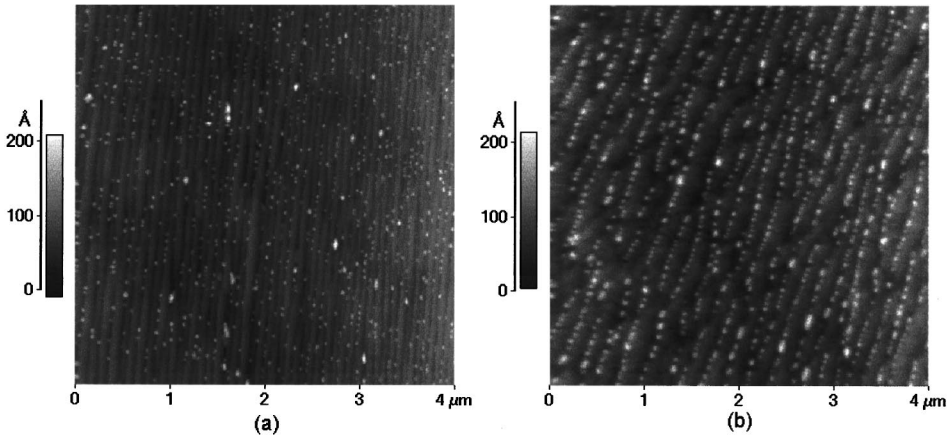

FIG. 3. AFM images of 2 ML InAs films grown on InP buffer with periodical multiterrace corrugations on (a) *A* surface and (b) *C* surface, respectively. $\Delta \mathbf{t}$ is 120 s (scan size, $4\times4\ \mu m^2$).

the other hand, are isotropic in shape with smaller lateral dimensions than those at the *A* surface and more evenly distributed on the surface.

While on *A* substrates the increase in the time interval between the InAs film and the InP cap layer deposition determined the appearance of 3D islands, for the samples on *C* substrates it implied a marked increase in island size. The comparison between Figs. 2(b) and 2(d) shows that the islands formed on the *C* surface increased as $\Delta \mathbf{t}$ was increased from 45 to 120 s, typical dimensions being 4 and 12 nm height and 40 nm and 65 nm of diameter, respectively.

The formation of 3D islands on misoriented substrates and the accumulation of InAs at the step edges on nominal substrates show that the presence of steps strongly affects the islanding process and determines the island characteristics—shape and spatial distribution. Besides that, the observation of 3D islands at the early stages of InAs deposition for samples grown on *B* and *C* surfaces, i.e., surfaces in which *B* steps are present, reinforces the idea that this type of step is more efficient to initiate islanding, than other types of steps. As we have previously reported, not only the step profiles (*B* steps are more kinked than *A* steps) but also the direction along which terraces run in the different types of surface can modify the distribution of surface adatoms along them.[19]

Our results clearly indicate that the presence of steps on misoriented substrates alters islanding. The fact that this process starts earlier on misoriented substrates at 500 °C, while the increase in size of the islands occurs after deposition suggests the existence of a microscopic dependence of surface diffusion on surface steps. This behavior has also been attributed to a more effective barrier for misoriented substrates than on the nominal ones, due to the higher density of steps on their surfaces. The results suggest that both the temperature and *B*-type steps favor the achievement, by the at-

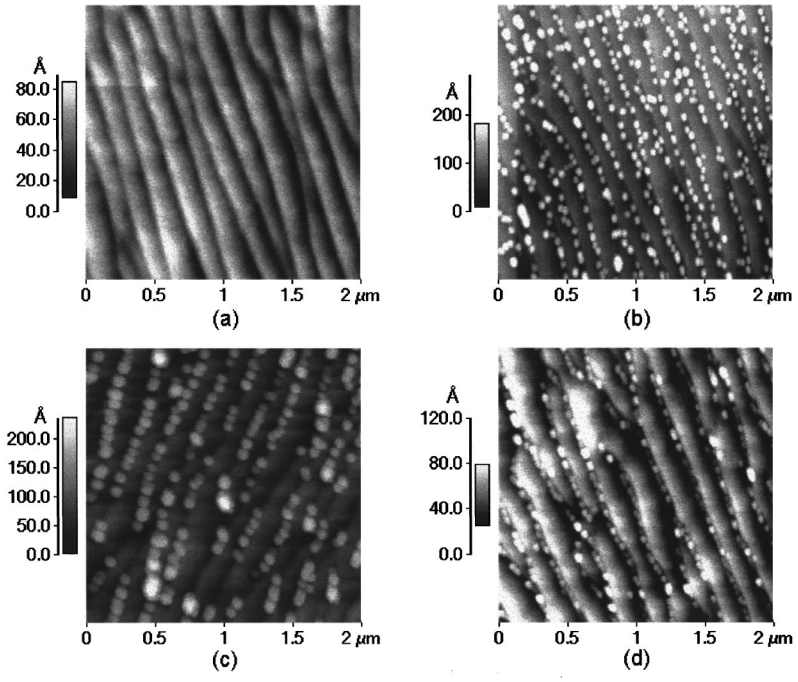

FIG. 4. (a) AFM images of the InP buffer with periodical multiterrace structure grown on *C* surface. AFM images of 2 ML InAs films grown on the InP buffer (b) with no InP cap layer, (c) $\Delta \mathbf{t}=120$ s, and (d) $\Delta \mathbf{t}=45$ s. Scan sizes are all $2\times2\ \mu m^2$.

oms, of a more energetically stable state through islanding. The 3D islands formed at growth temperature can, therefore, evolve in two steps: increasing in size and coarsening, favoring the eventual formation of larger, more stable islands. In this sense, the cooldown procedure we devised consists in suppressing the InAs surface redistribution by choosing the time for deposition of the InP cap layer. This process inhibits coarsening and allows the control of island sizes.

In order to study the influence of morphology on the islanding process, 2 ML-thick InAs films were deposited on the InP surface with periodic corrugation. Figure 3 shows the AFM images of the samples with $\Delta \mathbf{t} = 120$ s on (a) *A* and (b) *B* surfaces. In the first, the density of islands is about $50/\mu m^2$ and they are unevenly distributed along the multiatomic steps, while in the latter the island density is $100/\mu m^2$ and are more uniformly distributed on the surface. Contrary to what has been reported about $In_xGa_{1-x}As$ deposited on similar multiatomic structures on GaAs,[15,16] our results show the 3D InAs island density and spatial distribution present a remarkable dependence with the direction of the misorientation of vicinal (2° off) surfaces.

For these types of samples we will focus our discussion on those grown on *C* surfaces for two reasons: more uniform islands previously observed in this type of surface and provision of a more regular corrugation with *B* steps than other substrates. In Fig. 4(a) we show the AFM images of the InP corrugated buffer layer on the top of which the InAs films were deposited. The multiterrace structures are periodically arranged 180–200 nm from each other and their height is 5–6 nm. The AFM image of the InAs film cooled down to room temperature under AsH_3 flux is shown in Fig. 4(b). This image shows the remarkable alignment of the uniform self-assembled islands along the edge of the corrugation. Figures 4(c) and 4(d) present the AFM results for samples with $\Delta \mathbf{t} = 120$ and 45 s, respectively. Although the islands present a clear difference in size in the first two samples [Figs. 4(b) and 4(c)], it is when $\Delta \mathbf{t}$ is decreased to 45 s that the effect of the InP cap layer is more clearly noticed. For the $\Delta \mathbf{t} = 45$ s samples it can be observed that the islands are lower than the top of the corrugation.

The histograms for island height distribution of these samples, shown in Fig. 5, confirm this behavior. The height distributions for the samples with $\Delta \mathbf{t} = 45$, 120, and for that in which no InP cap was deposited are shown in Figs. 5(a), 5(b), and 5(c), respectively. The mean height increases varied from 3.5 ± 0.7 nm to 12.5 ± 3.5 nm as $\Delta \mathbf{t}$ increased. The low number of islands presented for the sample with $\Delta \mathbf{t} = 45$ s is due to the difficulty to perform precise measurements of the island dimensions caused by the small separation between each other.

At this point it is important to notice that, in our samples, the InAs layer was estimated to have a thickness that is under or approximately the critical value to islanding.[20,21] For the InAs samples grown on the corrugated InP surface we observe that islanding occurs earlier at the bottom of the (411) sidewalls. This result may be interpreted based on observations made for samples where lattice-matched $In_xGa_{1-x}As$ was deposited on the same type of corrugated InP surface. A larger thickness at the bottom of the corrugation was observed,[22] which can be attributed to different incorporation—due to irregularities along the (411) side

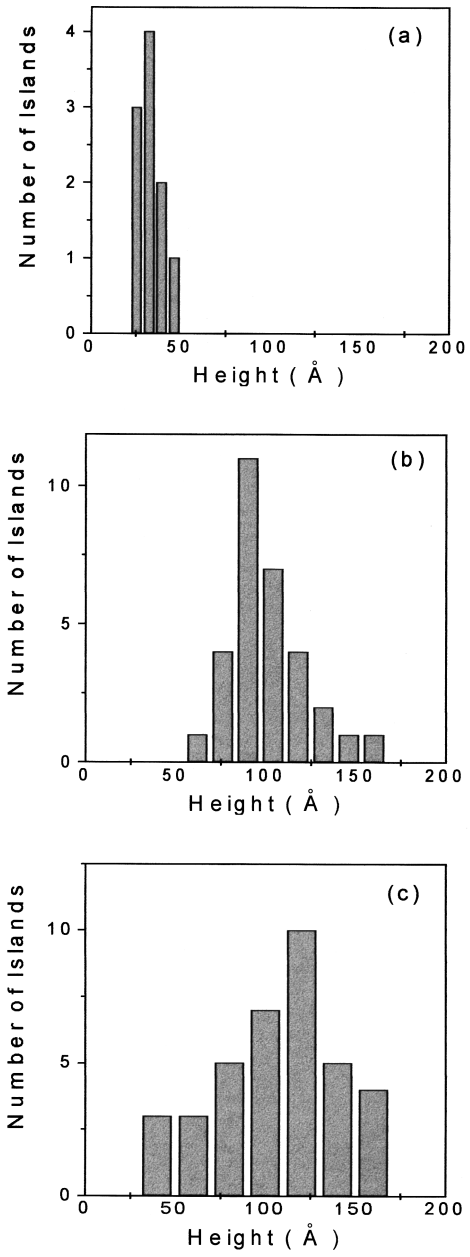

FIG. 5. Height distribution of InAs islands (2 ML deposited on corrugated buffer) for samples with (a) $\Delta \mathbf{t} = 45$ s, (b) 120 s, and (c) with no cap layer.

walls—and diffusion rates when different facets are present on the surface.[23,24] In this sense we assume that the InAs thickness approaches the critical value earlier in this region of the surface.

Surface energetics also indicates an earlier transition to islanding on the (100) than on (411) facets. Tersoff and Tromp[25] have proposed that there is an energy barrier for the formation of islands that depends on the difference between the free energies of the surfaces involved. In experiments with growth on patterned substrates[26] or under kinetically limited conditions,[27] it has been observed that (111) and (411) planes tend to form wherever there is a break in symmetry in (100) surfaces. This indicates that $\Gamma_{(411)}$ (sidewalls) is higher than $\Gamma_{(100)}$ (terraces) and that the energy barrier would, thus, be first overcome at the bottom of the corruga-

tion. The existence of a different crystallographic facet on the surface, however, is not a primary condition to favor islanding.

The islanding process is then assumed to initiate at the bottom of the corrugation and the surface atoms diffuse to the closest island, increasing its size. Provided the substrate temperature is kept high for enough time, the surface atoms will diffuse or be driven to the region where accumulation is favored. Islanding freeze out occurs if some islanding suppressing effect is introduced, as, for example, the deposition of a cap layer. A delay time for the development of the islands after the deposition of the strained layer has been reported,[9] while a low growth rate is one of the conditions to achieve the vertical alignment of InAs in multilayered InAs/GaAs.[10] In our samples, the InAs/InP system is given temperature and enough time to reach the energetically more favorable state. The surface diffusion activated during the sample cooldown [Fig. 3(a)] promotes an increase in the island sizes.

In summary, the idea that the formation of the islands is a more energetically favorable state is confirmed by our results. At high temperatures the surface kinetics of the atoms in the film gives rise to a coarsening process in which the control of the uniformity in island size has proved more difficult to achieve. In the controlled cooling procedure under AsH_3 flux, the departure from growth temperature provides the transition to a lower-energy configuration through islanding while it still allows the islands to increase in size. The understanding of these processes has provided means to obtain systems of InAs islands with controlled and well-defined characteristics so that InAs/InP structures with periodic spatial distribution can be achieved in a single step of growth.

The authors wish to thank P. A. Schulz and R. B. Martins for fruitful discussions. This work was financially supported by CNPq, FAPESP, FINEP, and Telebras (Brazil).

[1] R. Notzel, Semicond. Sci. Technol. **11**, 1365 (1996), and references therein.
[2] Y. Arakawa and H. Sakaki, Appl. Phys. Lett. **40**, 939 (1982); H. Sakaki, J. Appl. Phys. **28**, L314 (1989).
[3] K. Kash, J. Lumin. **46**, 69 (1990).
[4] D. J. Eaglesham and M. Cerulo, Phys. Rev. Lett. **64**, 1943 (1990).
[5] J. M. Moison, F. Houzay, F. Barthe, L. Leprince, E. André, and O. Vatel, Appl. Phys. Lett. **64**, 196 (1994).
[6] J. M. Gérard, J. B. Génin, J. Lefebvre, J. M. Moison, N. Lebouché, and F. Barthe, J. Cryst. Growth **150**, 351 (1995).
[7] R. Leonelli, C. A. Tran, J. L. Brebner, J. T. Graham, R. Tabti, R. A. Masut, and S. Charbonneau, Phys. Rev. B **48**, 11 135 (1993).
[8] A. Madhukar, Q. Xie, P. Chen, and A. Konkar, Appl. Phys. Lett. **64**, 2727 (1994).
[9] N. Carlsson, K. Georgsson, L. Montelius, L. Samuelson, W. Seifert, and R. Wallenberg, J. Cryst. Growth **156**, 23 (1995).
[10] J. Tersoff, C. Teichert, and M. G. Lagally, Phys. Rev. Lett. **76**, 1675 (1996).
[11] Q. Xie, A. Madhukar, P. Chen, and N. P. Kobayashi, Phys. Rev. Lett. **75**, 2542 (1995).
[12] D. Leonard, K. Pond, and P. M. Petroff, Phys. Rev. B **50**, 11 687 (1994).
[13] S. P. DenBaars, C. M. Reaves, V. Bressler-Hill, S. Varma, W. H. Weinberg, and P. M. Petroff, J. Cryst. Growth **145**, 721 (1994).
[14] D. S. Mui, D. Leonard, L. A. Coldren, and P. M. Petroff, Appl. Phys. Lett. **66**, 1620 (1995).
[15] M. Kitamura, M. Nishioka, J. Oshinowo, and Y. Arakawa, Appl. Phys. Lett. **66**, 3663 (1995).
[16] M. Kitamura, M. Nishioka, J. Oshinowo, and Y. Arakawa, Jpn. J. Appl. Phys., Part 1 **34**, 4376 (1995).
[17] M. Sopanen, H. Lipsanen, and J. Ahopelto, Appl. Phys. Lett. **67**, 3768 (1995).
[18] M. A. Cotta, R. A. Hamm, T. W. Staley, S. N. G. Chu, R. Hull, L. R. Harriot, M. B. Panish, and H. Temkin, Phys. Rev. Lett. **70**, 4106 (1993).
[19] M. A. Cotta, C. A. C. Mendonça, E. A. Meneses, and M. M. G. Carvalho, Surf. Sci. **388**, 84 (1997).
[20] C. W. Snyder, B. G. Orr, D. Kressler, and L. M. Sander, Phys. Rev. Lett. **66**, 3032 (1991).
[21] M. A. Cotta, C. A. C. Mendonça, K. M. Ito-Landers, M. M. G. Carvalho, and R. B. Martins, *Proceedings of the 8th International Conference on Indium Phosphide and Related Materials* (IEEE, Inc., Schwäbisch Gmünd, 1996).
[22] M. A. Cotta, R. A. Hamm, S. N. G. Chu, L. R. Harriot, and H. Temkin, J. Appl. Phys. **75**, 630 (1994).
[23] Y. Morishita, Y. Nomura, S. Goto, Y. Katayama, and T. Isu, Surf. Sci. **267**, 17 (1992).
[24] F. S. Turco, M. C. Tamargo, D. M. Hwang, R. E. Nahory, J. Werner, K. Kash, and E. Kapon, Appl. Phys. Lett. **56**, 72 (1990).
[25] J. Tersoff and R. M. Tromp, Phys. Rev. Lett. **70**, 2782 (1993).
[26] W. Tang and A. Y. Cho, Appl. Phys. Lett. **30**, 293 (1977).
[27] M. A. Cotta, R. A. Hamm, S. N. G. Chu, R. Hull, L. R. Harriot, and H. Temkin, Mater. Sci. Technol. **B30**, 137 (1995).